

Supporting Information

for

Stability of Star-shaped RAFT Polystyrenes under Mechanical and Thermal Stress

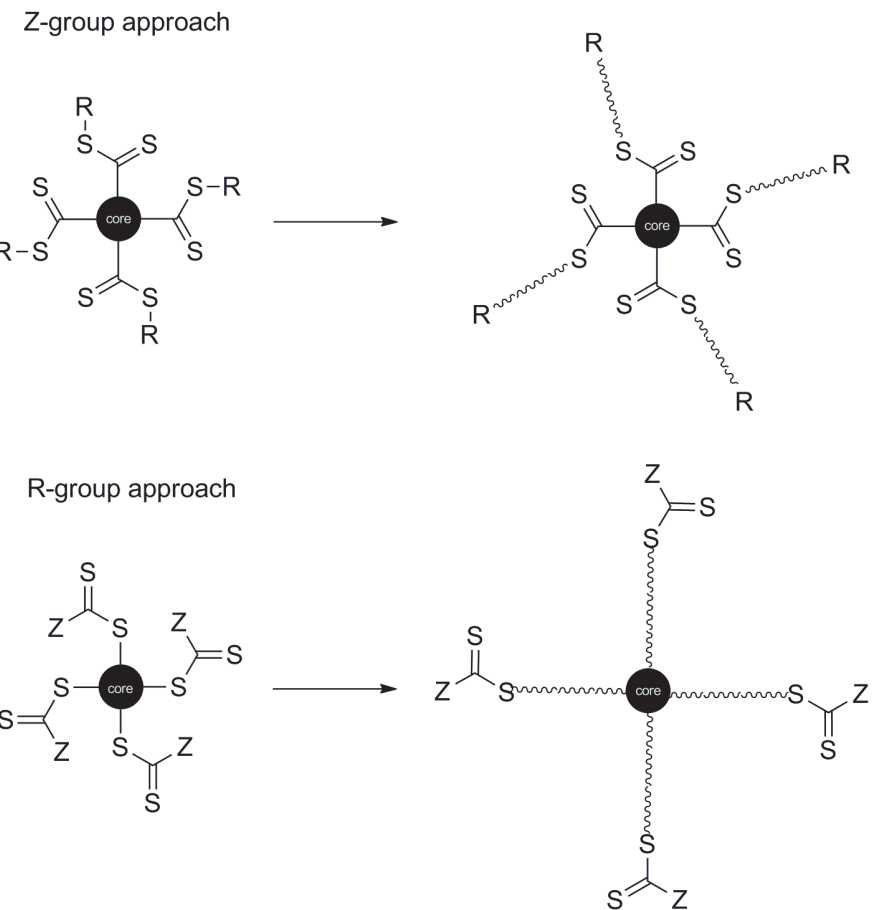
Ozcan Altintas,^{1,2,3} Mahdi Abbasi,² Kamran Riazi,² Anja S. Goldman,^{1,3} Nico Dingenouts,² Manfred Wilhelm^{2*} and Christopher Barner-Kowollik^{1,3*}

¹Preparative Macromolecular Chemistry, Institut für Technische Chemie und Polymerchemie, Karlsruhe Institute of Technology (KIT), Engesserstr. 18, 76128 Karlsruhe, Germany.

²Polymeric Materials, Institut für Technische Chemie und Polymerchemie, Karlsruhe Institute of Technology (KIT), Engesserstr. 18, 76128 Karlsruhe, Germany.

³Institut für Biologische Grenzflächen, Karlsruhe Institute of Technology (KIT), Hermann-von-Helmholtz Platz 1, 76344 Eggenstein-Leopoldshafen, Germany.

*To whom correspondence should be addressed
E-mail: manfred.wilhelm@kit.edu
E-mail: christopher.barner-kowollik@kit.edu



Scheme S1. Synthesis of star polymers via the RAFT process following a R- or Z-group approach. Note that the Z-group approach is generally preferred – being unique to the RAFT process – as it avoids the formation star-star coupling, as the core never carries the radical function.

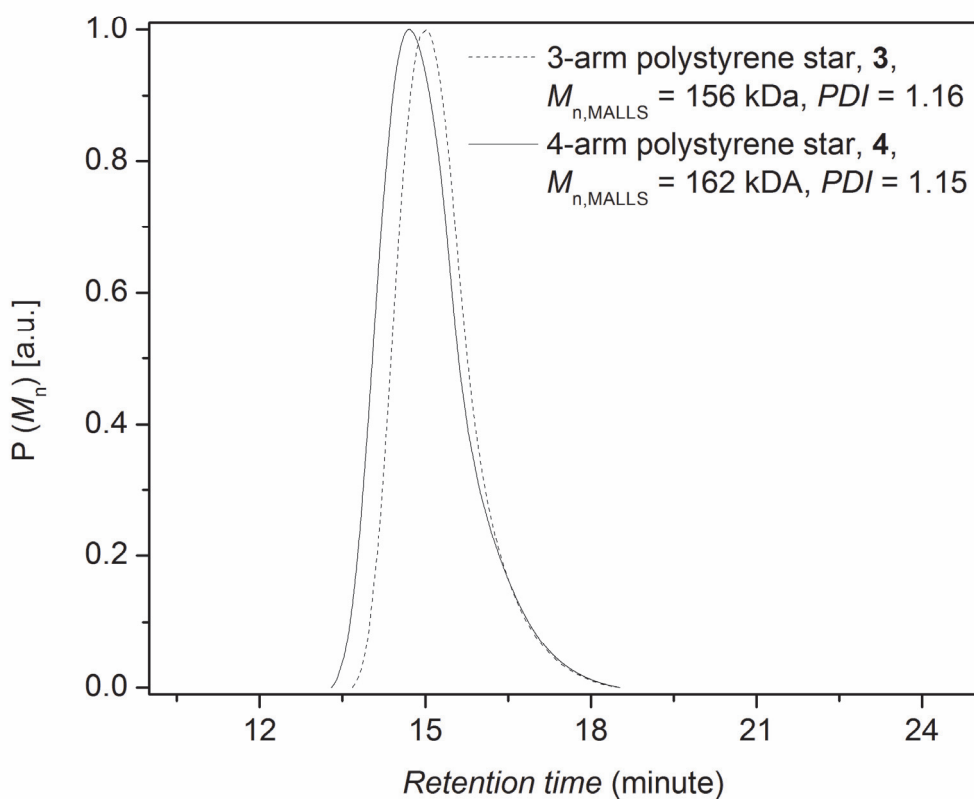


Figure S1. SEC traces of trithiocarbonate core-functional 3-arm star-shaped polystyrene **3** and 4-arm star-shaped polystyrene **4** in THF employed in the degradation and extrusion experiments prior to any stress (MALLS detection) determined via visco detection.

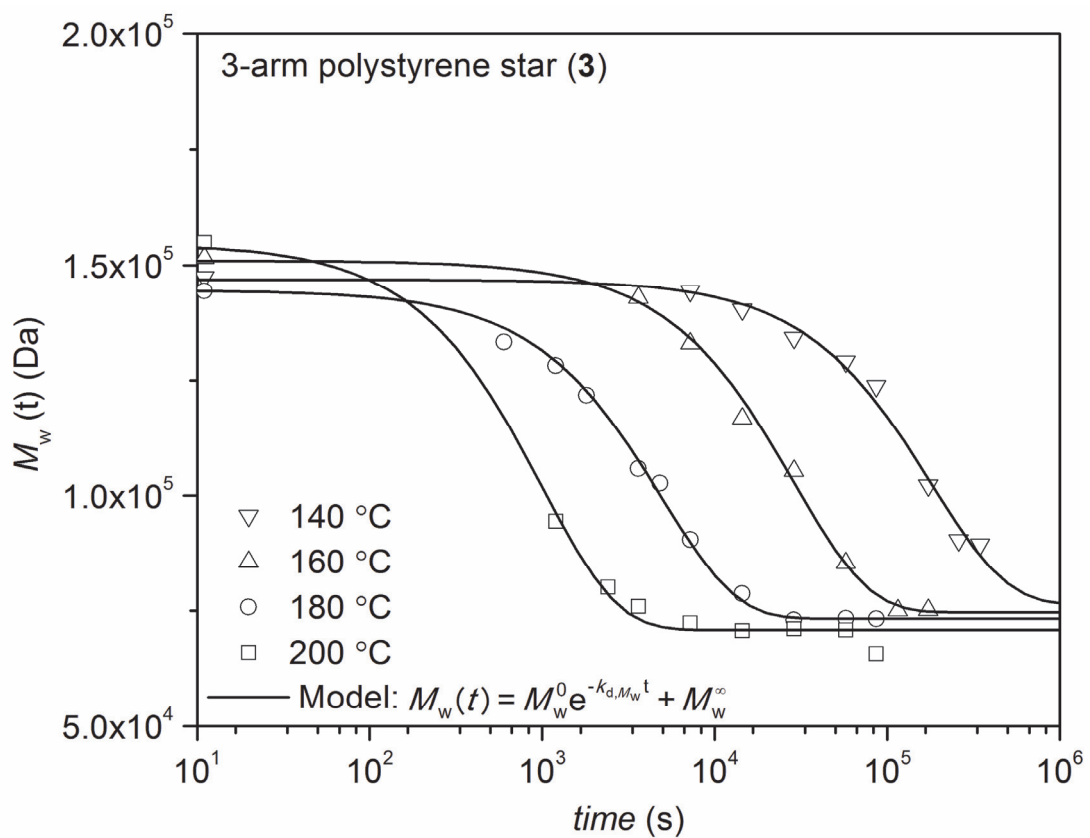


Figure S2. Weight-average molecular weight, $M_w(t)$, as a function of time at variable temperatures for the degradation of trithiocarbonate core functional 3-arm star polystyrene **3**. The scatter in the starting molecular weights is due their individual SEC reanalysis for each temperature run (featuring an error of close to 12%). The time starts at 10 s as this period represents the sampling time of the experiment.

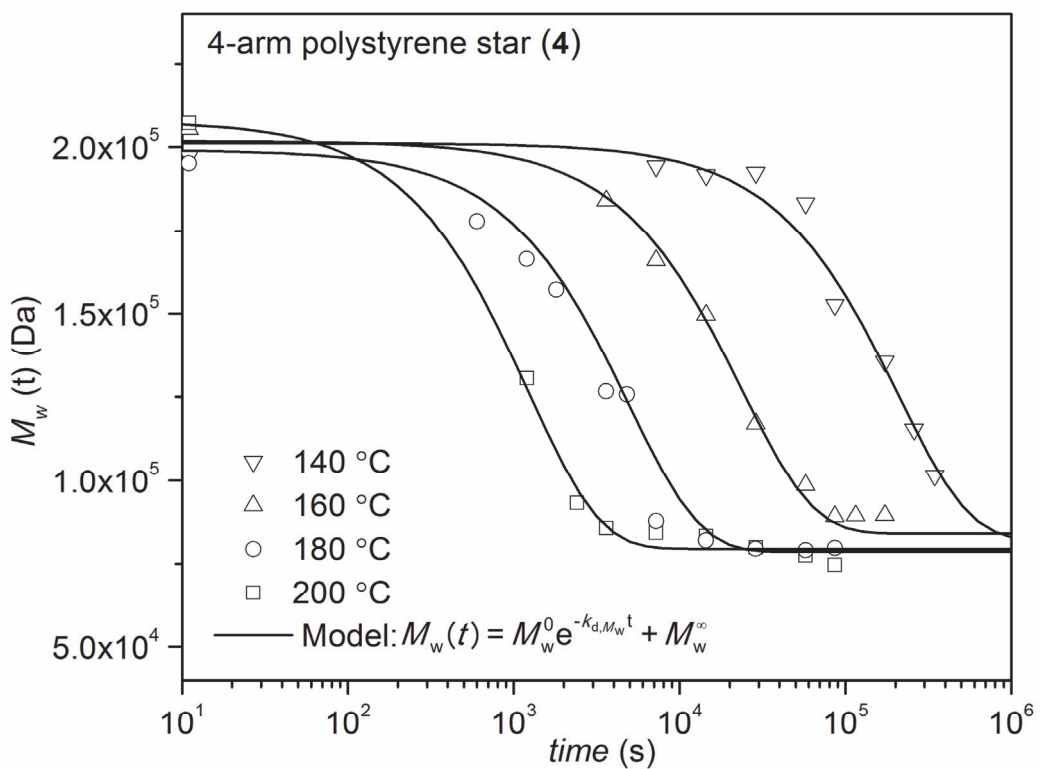


Figure S3. Weight-average molecular weight, $M_w(t)$, as a function of time at variable temperatures for the degradation of trithiocarbonate core functional 4-arm star polystyrene **4**. The scatter in the starting molecular weights is due their individual SEC reanalysis for each temperature run (featuring an error of close to 12%). The time starts at 10 s as this period represents the sampling time of the experiment.

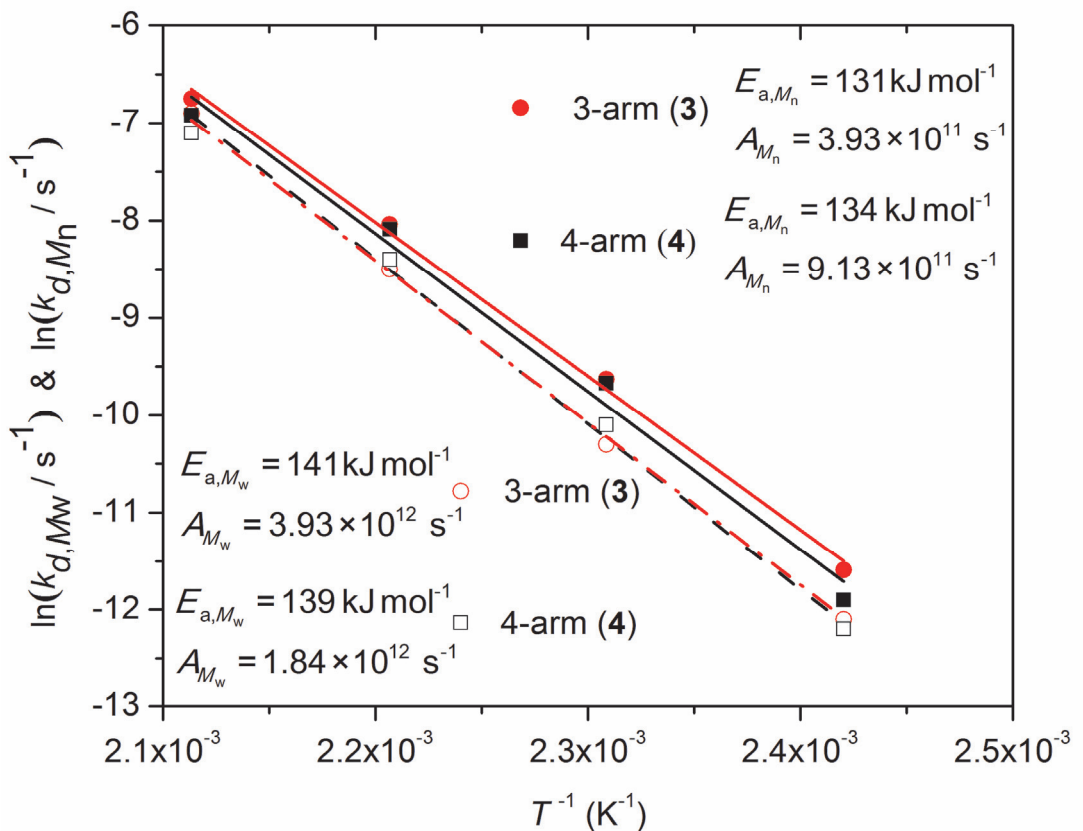


Figure S4. Arrhenius plots of the rate coefficient for the cleavage of Z-type RAFT based 3-arm star-shaped polystyrenes (**3**) and 4-arm star-shaped polystyrenes (**4**) based on M_n (filled symbols) and M_w (open symbols) featuring trithiocarbonate core-functionalities in an argon atmosphere.

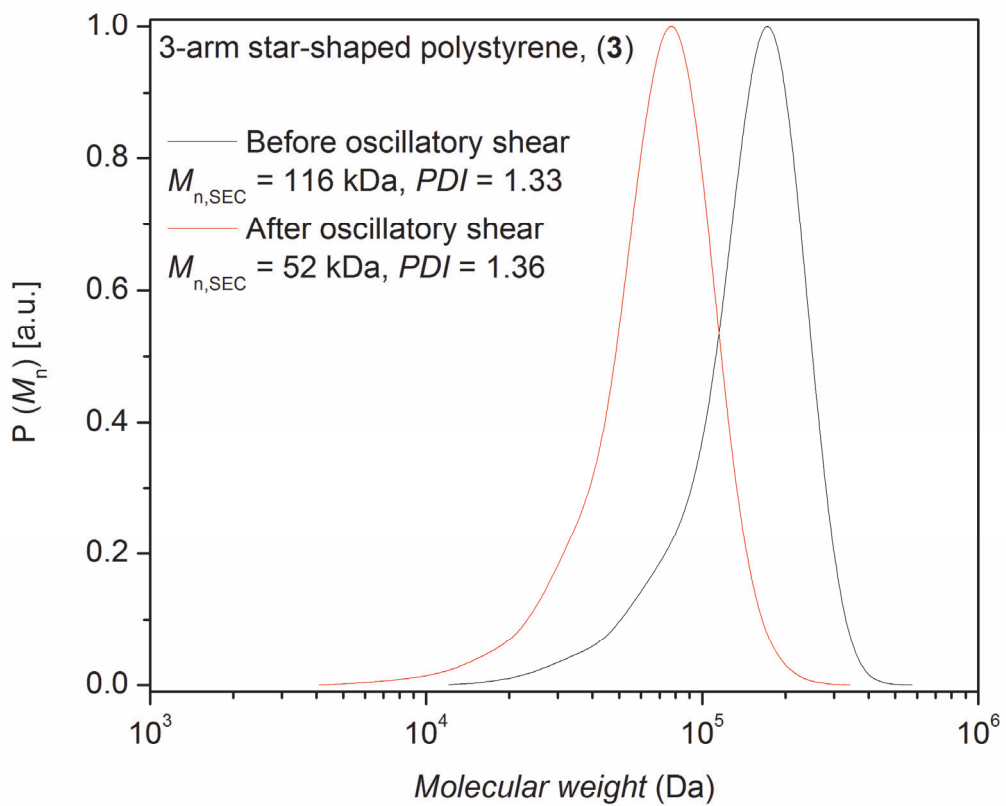


Figure S5. SEC trace of the trithiocarbonate core-functional 3-arm star-shaped polystyrene (3) before and after 8 hours applying oscillatory shear with $\omega/2\pi = 0.05$ Hz and $\gamma_0 = 0.25$ strain amplitude at 180 °C in a nitrogen atmosphere via DRI detector.

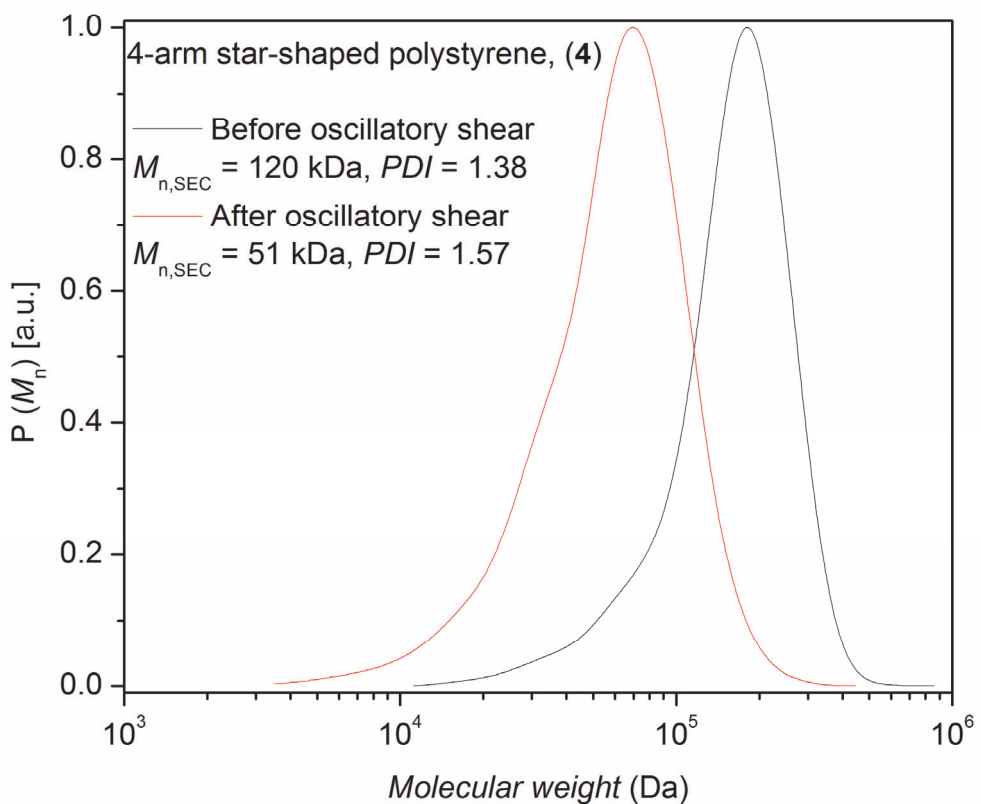


Figure S6. SEC trace of the trithiocarbonate core-functional 4-arm star-shaped polystyrene (4) before and after applying oscillatory shear with $\omega/2\pi = 0.05 \text{ Hz}$ and $\gamma_0 = 0.25$ strain amplitude at 180°C in a nitrogen atmosphere.

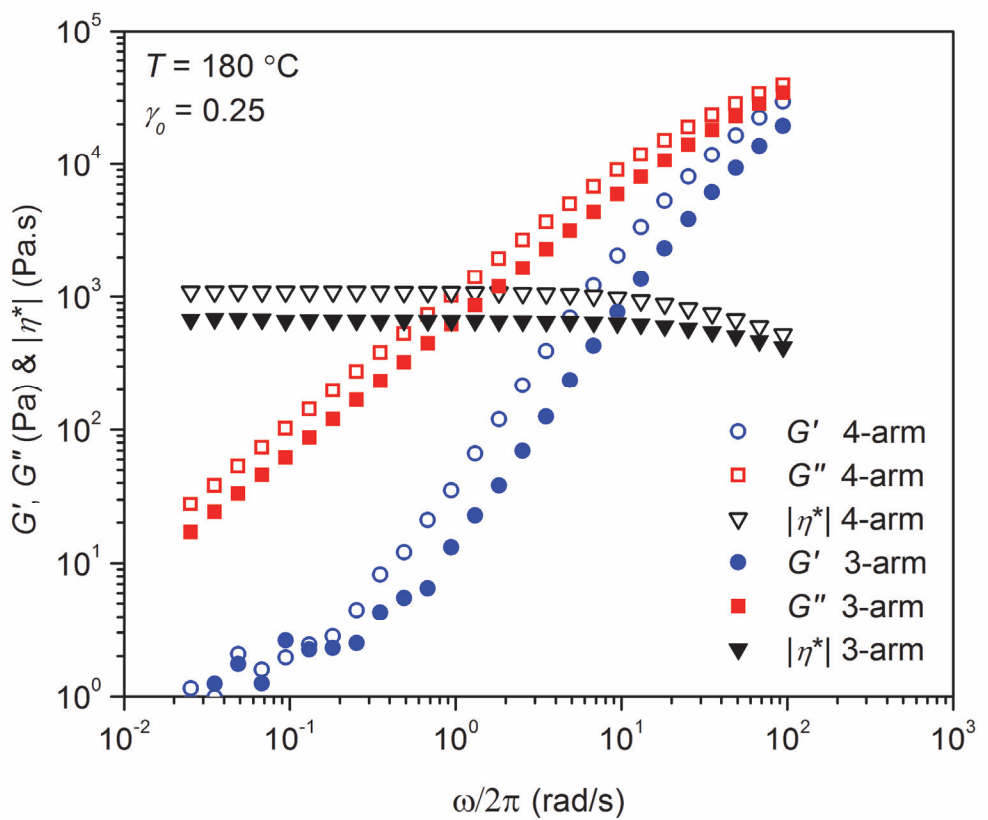


Figure S7. Dynamic frequency sweep test of star polystyrenes at the end of dynamic time sweep test after 8 hours (refer to Figure 8 in the main text) in rheometer.

Appendix I

Weight-average molecular weight dependency of zero shear viscosity during the cleavage process

Zero shear viscosity and weight average molecular weight of designed star polystyrenes show an exponential time dependence during the core cleavage process in the following form:

$$M_w(t) = M_w^0 e^{-k_{d,M_w} t} + M_w^\infty \quad (\text{I1})$$

$$\eta_0(t) = \eta_0^0 e^{-k_{D0} t} + \eta_0^1 e^{-k_{D1} t} + \eta_0^\infty \quad (\text{I2})$$

Neglecting the effect of arm degradation, second part in the right hand of Eq. I2, and rearrangement of these equations result in:

$$\frac{M_w(t) - M_w^\infty}{M_w^0} = e^{-k_{d,M_w} t} \quad (\text{I3})$$

$$\frac{\eta_0(t) - \eta_0^{\infty,c}}{\eta_0^0} \approx e^{-k_{D0} t} \quad (\text{I4})$$

A natural logarithm of both sides results:

$$\ln\left(\frac{M_w(t) - M_w^\infty}{M_w^0}\right) = -k_{d,M_w} t \quad (\text{I5})$$

$$\ln\left(\frac{\eta_0(t) - \eta_0^{\infty,c}}{\eta_0^0}\right) \approx -k_{D0} t \quad (\text{I6})$$

Dividing Eq. (I6) to Eq. (I5) results in:

$$\ln \frac{\eta_0(t) - \eta_0^{\infty,c}}{\eta_0^0} / \ln \frac{M_w(t) - M_w^\infty}{M_w^0} \approx \frac{k_{D0}}{k_{d,M_w}} \quad (\text{I7})$$

Consequently:

$$\frac{\eta_0(t) - \eta_0^{\infty,c}}{\eta_0^0} \approx \left(\frac{M_w(t) - M_w^\infty}{M_w^0} \right)^{k_{D0}/k_{d,M_w}} \quad (\text{I8})$$

The power law dependency of the zero shear viscosity, η_0 , of the weight average molecular weight, $\eta_0 = kM_w^\alpha$, and its power exponent, α , is of significant importance for rheological properties. The exponent α reads 3.4 for linear polymers above the critical molecular weight, $M_c \approx 3M_e$. With respect to these criteria, a rearrangement of Eq. (I8) and analytical molecular weight derivative of zero shear viscosity is developed:

$$\eta_0(t) \approx \eta_0^0 \left(\frac{M_w(t) - M_w^\infty}{M_w^0} \right)^{k_{D0}/k_{d,Mw}} + \eta_0^{\infty,c} \quad (\text{I9})$$

$$d\eta_0(t)/dM_w(t) \approx \frac{k_{D0}}{k_{d,Mw}} \frac{\eta_0^0}{M_w^0} \left(\frac{M_w(t) - M_w^\infty}{M_w^0} \right)^{k_{D0}/k_{d,Mw}-1} \quad (\text{I10})$$

On the other hand:

$$d \ln M_w(t) = \frac{dM_w(t)}{M_w(t)} \quad (\text{I11})$$

$$d \ln \eta_0(t) = \frac{d\eta_0(t)}{\eta_0(t)} \quad (\text{I12})$$

Combining the Eq. (I10) – (I12) results in:

$$\frac{d \ln \eta_0(t)}{d \ln M_w(t)} \approx \frac{k_{D0}}{k_{d,Mw}} \frac{M_w(t)}{\eta_0(t)} \frac{\eta_0^0}{M_w^0} \left(\frac{M_w(t) - M_w^\infty}{M_w^0} \right)^{k_{D0}/k_{d,Mw}-1} \quad (\text{I13})$$

Rearrangement of Eq. (I13) results in:

$$\frac{d \ln \eta_0(t)}{d \ln M_w(t)} \approx \frac{k_{D0}}{k_{d,Mw}} \frac{M_w(t)}{\eta_0(t)} \frac{\eta_0^0}{M_w^0} \left(\frac{M_w(t) - M_w^\infty}{M_w^0} \right)^{k_{D0}/k_{d,Mw}} / \left(\frac{M_w(t) - M_w^\infty}{M_w^0} \right) \quad (\text{I14})$$

Finally, inserting the Eq. (I8) in Eq. (I14) gives:

$$\frac{d \ln \eta_0(t)}{d \ln M_w(t)} \approx \frac{k_{D0}}{k_{d,Mw}} \frac{M_w(t)}{\eta_0(t)} \frac{\eta_0^0}{M_w^0} \left(\frac{\eta_0(t) - \eta_0^{\infty,c}}{\eta_0^0} \right) / \left(\frac{M_w(t) - M_w^\infty}{M_w^0} \right) \quad (\text{I15})$$

$$\frac{d \ln \eta_0(t)}{d \ln M_w(t)} \approx \frac{k_{D0}}{k_{d,Mw}} \frac{M_w(t)}{\eta_0(t)} \left(\frac{\eta_0(t) - \eta_0^{\infty,c}}{M_w(t) - M_w^\infty} \right) \quad (\text{I16})$$